AUXILIARY BEAM PAIR DESIGN IN MMWAVE CELLULAR SYSTEMS WITH HYBRID PRECODING AND LIMITED FEEDBACK

Dalin Zhu, Junil Choi, and Robert W. Heath Jr.

Department of Electrical and Computer Engineering
The University of Texas at Austin
Email: {dalin.zhu, junil.choi, rheath}@utexas.edu

ABSTRACT

Auxiliary beam pairs are proposed in millimeter-wave cellular systems for closed-loop hybrid precoding. Pairs of custom designed analog beams are formed to help acquire channel information. It is shown via simulations that auxiliary beam pairs have lower complexity and better achievable rates with a moderate amount of feedback, compared to conventional beam training methods.

***Index Terms*—** hybrid analog and digital precoding, mmWave, auxiliary beam pair, limited feedback, MIMO

1. INTRODUCTION

The millimeter wave (mmWave) band holds promise for providing high data rates in cellular systems [1]-[4]. The small carrier wavelengths at mmWave frequencies enable synthesis of compact antenna arrays, providing large beamforming gains to enable favorable received power. The large antenna arrays can also be used in a multiple-input multiple-output (MIMO) configuration to support the transmission of multiple data streams, and to further improve the spectral efficiency. Hybrid analog and digital precoding has become a means of exploiting both beamforming and spatial multiplexing gains in hardware constrained mmWave cellular systems [5]-[11]. Many of the previous hybrid precoding solutions require a lot of training to find the best analog and baseband precoders [8, 9, 10]. Further work is therefore needed to optimize the hybrid precoding technique for practical deployment with feasible implementation complexity.

In this paper, we consider the optimization of analog precoding through auxiliary beam pairs (ABPs) to facilitate closed-loop hybrid precoding. In the proposed technique, the transmitter probes pairs of specially designed analog beams towards certain angular directions to help the receiver acquire channel information. After receiving the beamformed signals, the receiver calculates a set of ratio metrics and feeds their quantized versions back to the transmitter. Based on the feedback, the transmitter adjusts the corresponding beamforming directions and performs data transmissions via hybrid precoding.

Construction of pairs of beams is previously employed in amplitude monopulse radar like systems to improve the estimation accuracy of the direction of arrival [12]-[15]. To the best of our knowledge, this paper is the first work that considers implementing the well-structured beam pairs in mmWave cellular systems to enable closed-loop hybrid precoding. It is shown via analysis and simulation results that the proposed auxiliary beam pairs based hybrid precoding design exhibits comparable data rate performance to the grid-of-beam (GoB) based method [9] under a moderate amount of feedback bits, but with reduced implementation complexity.

We use the following notations: $\boldsymbol{A}$ is a matrix; $\mathbf{a}$ is a vector; a is a scalar; $(\cdot)^{\mathrm{T}}$ and $(\cdot)^*$ denote transpose and conjugate transpose, respectively; $\|\boldsymbol{A}\|_{\mathrm{F}}$ is the Frobenius norm of $\boldsymbol{A}$; $\boldsymbol{I}_N$ is the $N \times N$ identity matrix; $\mathbf{0}_N$ denotes the $N \times 1$ vector whose entries are all zeros; $\mathcal{CN}(\mathbf{a}, \boldsymbol{A})$ is a complex Gaussian vector with mean $\mathbf{a}$ and covariance $\boldsymbol{A}$.

2. SYSTEM MODEL

We consider a narrow band MIMO system with a hybrid precoding structure as shown in Fig. 1, in which a transmitter equipped with N_{tot} transmit antennas and N_{RF} radio frequency (RF) chains transmits N_{S} data streams to a receiver equipped with M_{tot} receive antennas and M_{RF} RF chains. Here, $N_{\mathrm{S}} \leq \min(N_{\mathrm{RF}}, M_{\mathrm{RF}})$. Each antenna subarray is controlled by a single RF chain. If the number of antenna elements per antenna subarray at the transmitter and receiver are N_{Sub} and M_{Sub} respectively, we have $N_{\mathrm{tot}} = N_{\mathrm{RF}} N_{\mathrm{Sub}}$ and $M_{\mathrm{tot}} = M_{\mathrm{RF}} M_{\mathrm{Sub}}$. Denoting by $\mathbf{x}$ the $N_{\mathrm{S}} \times 1$ vector of symbols such that $\mathbb{E}[\mathbf{x}^*\mathbf{x}] = P$, and by $\mathbf{y}$ the $N_{\mathrm{S}} \times 1$ vector of symbols received across the receive antennas after analog and baseband combining, the received signal is

$$\mathbf{y} = \boldsymbol{W}_{\mathrm{BB}}^* \boldsymbol{W}_{\mathrm{RF}}^* \boldsymbol{H} \boldsymbol{F}_{\mathrm{RF}} \boldsymbol{F}_{\mathrm{BB}} \mathbf{x} + \mathbf{n}, \tag{1}$$

where $\mathbf{n} \sim \mathcal{CN}(\mathbf{0}_{M_{\mathrm{tot}}}, \sigma^2 \boldsymbol{I}_{M_{\mathrm{tot}}})$ is a noise vector, $\boldsymbol{H}$ represents the $M_{\mathrm{tot}} \times N_{\mathrm{tot}}$ narrow band MIMO channel, which can be formulated according to the ray-cluster based spatial channel model given in [16], $\boldsymbol{F}_{\mathrm{RF}}$ is the $N_{\mathrm{tot}} \times N_{\mathrm{RF}}$ analog precoding matrix at the transmitter such that $\|\boldsymbol{F}_{\mathrm{RF}}\|_{\mathrm{F}}^2 = 1$,

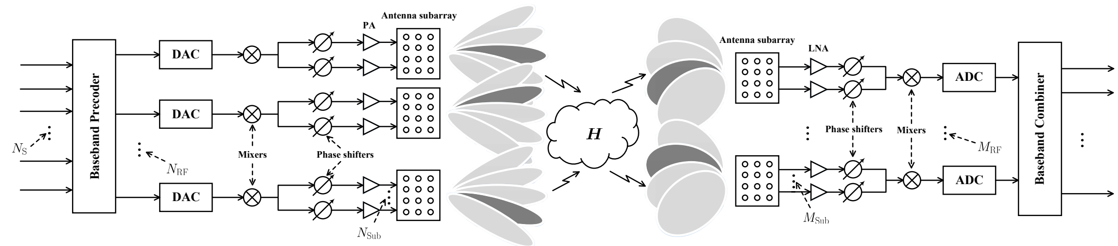

Fig. 1. A transceiver structure of hybrid precoding based narrow band MIMO systems.

$\boldsymbol{F}_{\rm BB}$ is the $N_{\rm RF}\times N_{\rm S}$ digital baseband precoding matrix at the transmitter such that $\|\boldsymbol{F}_{\rm BB}\|_{\rm F}^2=1$, $\boldsymbol{W}_{\rm BB}$ and $\boldsymbol{W}_{\rm RF}$ respectively denote $M_{\rm RF}\times N_{\rm S}$ and $M_{\rm tot}\times M_{\rm RF}$ baseband and analog combining matrices under the power constraints of $\|\boldsymbol{W}_{\rm BB}\|_{\rm F}^2=1$ and $\|\boldsymbol{W}_{\rm RF}\|_{\rm F}^2=1$. Since each antenna subarray is connected to only one RF chain, $\boldsymbol{F}_{\rm RF}$ exhibits a block diagonal structure such that its non-zero diagonal entries are $N_{\rm Sub}\times 1$ constant-amplitude phase-only vectors. Assume the availability of channel state information, optimal analog precoder and combiner can be obtained via sparse reconstruction in mmWave MIMO systems [5, 6]. In this paper, we assume that the transmitter employs a uniform linear array (ULA). While arbitrary phase adjustment is possible at each antenna element [5]-[7], we further assume that the steering vector for the transmit antenna subarray is a function of a single phase [8, 9], results in

$$\boldsymbol{F}_{\rm RF}=\begin{bmatrix}\mathbf{a}_{\rm t}(\theta_1) & \mathbf{0}_{N_{\rm Sub}} & \cdots & \mathbf{0}_{N_{\rm Sub}}\\ \mathbf{0}_{N_{\rm Sub}} & \mathbf{a}_{\rm t}(\theta_2) & \cdots & \mathbf{0}_{N_{\rm Sub}}\\ \vdots & \vdots & \ddots & \vdots\\ \mathbf{0}_{N_{\rm Sub}} & \mathbf{0}_{N_{\rm Sub}} & \cdots & \mathbf{a}_{\rm t}\left(\theta_{N_{\rm RF}}\right)\end{bmatrix}, \tag{2}$$

where the i-th diagonal entry $\mathbf{a}_{\rm t}(\theta_i)$ represents the analog steering vector for the i-th transmit antenna subarray ($i=1,2,\cdots,N_{\rm RF}$) and θ_i is the corresponding steering angle. We further have,

$$\mathbf{a}_{\rm t}(\theta_i)=\frac{1}{\sqrt{N_{\rm Sub}}}\left[1,e^{j\epsilon_{\rm t}\sin(\theta_i)},\cdots,e^{j\epsilon_{\rm r}(N_{\rm Sub}-1)\sin(\theta_i)}\right]^{\rm T}, \tag{3}$$

where $\epsilon_{\rm t}=\frac{2\pi}{\lambda}d_{\rm t}$, λ represents the wavelength corresponding to the operating carrier frequency, and $d_{\rm t}$ is the inter-element distance of the antenna elements at the transmitter. The analog combining matrix $\boldsymbol{W}_{\rm RF}$ at the receiver can be similarly defined as $\boldsymbol{F}_{\rm RF}$.

3. ABPS DESIGN FOR HYBRID PRECODING

The basic design principles of auxiliary beam pair are first illustrated assuming: (i) single transmit antenna subarray, (ii) only one omni-directional antenna element is equipped at the receiver, i.e., $M_{\rm tot}=1$, and (iii) line-of-sight (LOS) channel condition. Extending the proposed auxiliary beam pairs

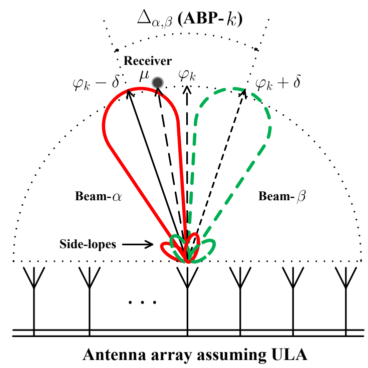

Fig. 2. An example of auxiliary beam pair containing beam-α and beam-β steering towards $\varphi_k-\delta$ and $\varphi_k+\delta$, respectively.

design to multiple subarrays is explained in the later of this section. Since the number of non-LOS (NLOS) components in mmWave channels is limited [17], they have negligible impacts on the performance of our proposed technique. Simulation results shown in Section 4 further validate our analysis. For simplicity, here, the index i of the transmit antenna subarray is omitted unless otherwise specified. Assuming that the transmitter employs a ULA, the transmit array response vector can therefore be denoted by $\mathbf{a}_{\rm t}(\bar{\theta})$, where $\bar{\theta}$ represents the angle-of-arrival (AoD). Denote by $\mu=\epsilon_{\rm t}\sin(\bar{\theta})$. As $\bar{\theta}\in\left[-\frac{\pi}{2},\frac{\pi}{2}\right]$ for a general setup, μ and $\bar{\theta}$ have a one-to-one correspondence. Hence, the array response vector for the transmitter can be expressed as

$$\mathbf{a}_{\rm t}(\mu)=\frac{1}{\sqrt{N_{\rm Sub}}}\left[1,e^{j\mu},\cdots,e^{j(N_{\rm Sub}-1)\mu}\right]^{\rm T}. \tag{4}$$

The transmitter forms pairs of custom designed analog beams within a given angular range. Fig. 2 shows one example of one auxiliary beam pair containing two analog beams. The plotted auxiliary beam pair is indexed by k (denote by ABP-k) such that $k\in\{1,2,\cdots,K\}$, where K represents the total number of formed auxiliary beam pairs. We denote the two analog beams in ABP-k by beam-α and beam-β, respectively. As can be seen from Fig. 2, the two beamforming vectors targeted, respectively, at the directions of $\varphi_k - \delta$ and $\varphi_k + \delta$ are expressed as

$$\boldsymbol{f}_\alpha(\delta, \varphi_k) = \frac{1}{\sqrt{N_{\text{Sub}}}} \left[1, e^{j(\varphi_k - \delta)}, \cdots, e^{j(N_{\text{Sub}}-1)(\varphi_k - \delta)}\right]^{\text{T}}, \tag{5}$$

and

$$\boldsymbol{f}_\beta(\delta, \varphi_k) = \frac{1}{\sqrt{N_{\text{Sub}}}} \left[1, e^{j(\varphi_k + \delta)}, \cdots, e^{j(N_{\text{Sub}}-1)(\varphi_k + \delta)}\right]^{\text{T}}. \tag{6}$$

Here, $\Delta_{\alpha,\beta} = [\varphi_k - \delta, \varphi_k + \delta]$ denotes the main probing range of beam-α and beam-β in ABP-k, where δ is the half of the range of the beamforming region for the transmitter. For simplicity, we set $\delta = \frac{2\ell\pi}{N_{\text{Sub}}}$ where $\ell = 1, \cdots, \frac{N_{\text{Sub}}}{4}$ is an integer allowing that $\delta \leq \frac{\pi}{2}$. Assume that the receiver is located within the main probing range of ABP-k, i.e., $|\mu - \varphi_k| \leq \delta$. Hence, the effective transmit beam-space channel gain can be calculated as

$$\chi_\alpha(k) = |\mathbf{a}_{\text{t}}^*(\mu)\boldsymbol{f}_\alpha(\delta, \varphi_k)|^2 \overset{(\circledast)}{=} \frac{\sin^2\left(\frac{N_{\text{Sub}}(\mu - \varphi_k)}{2}\right)}{N_{\text{Sub}}\left[\sin^2\left(\frac{\mu - \varphi_k + \delta}{2}\right)\right]}. \tag{7}$$

where $(\circledast)$ is obtained via $\left|\sum_{m=1}^{M} e^{-j(m-1)x}\right|^2 = \frac{\sin^2\left(\frac{Mx}{2}\right)}{\sin^2\left(\frac{x}{2}\right)}$, and by applying $\delta = \frac{2\ell\pi}{N_{\text{Sub}}}$. Similarly, the effective transmit beam-space channel gain of probing beam-β in ABP-k is derived as

$$\chi_\beta(k) = \frac{\sin^2\left(\frac{N_{\text{Sub}}(\mu - \varphi_k)}{2}\right)}{N_{\text{Sub}}\left[\sin^2\left(\frac{(\mu - \varphi_k - \delta)}{2}\right)\right]}. \tag{8}$$

Then, a ratio metric via the difference and the sum on $\chi_\alpha(k)$ and $\chi_\beta(k)$ can be obtained as [12]-[15]

$$\zeta_k = \frac{\chi_\alpha(k) - \chi_\beta(k)}{\chi_\alpha(k) + \chi_\beta(k)} = -\frac{\sin(\mu - \varphi_k)\sin(\delta)}{1 - \cos(\mu - \varphi_k)\cos(\delta)}. \tag{9}$$

As $|\mu - \varphi_k| \leq \delta$, it is easy to show that ζ_k is a monotonically decreasing function of $\mu - \varphi_k$ [12, 14]. We can therefore obtain the estimated AoD via the reverse function as

$$\hat{\mu} = \varphi_k - \arcsin\left(\frac{\zeta_k \sin(\delta) - \zeta_k\sqrt{1 - \zeta_k^2}\sin(\delta)\cos(\delta)}{\sin^2(\delta) + \zeta_k^2\cos^2(\delta)}\right). \tag{10}$$

If ζ_k is perfect, i.e., not impaired by noise, channel estimation error and quantization error, $\hat{\mu} = \mu$. The corresponding transmit array response vector can then be constructed as

$$\mathbf{a}_{\text{t}}(\hat{\theta}) = \frac{1}{\sqrt{N_{\text{Sub}}}} \left[1, e^{j\epsilon_{\text{r}}\sin(\hat{\theta})}, \cdots, e^{j\epsilon_{\text{r}}(N_{\text{Sub}}-1)\sin(\hat{\theta})}\right]^{\text{T}}, \tag{11}$$

with $\hat{\theta} = \arcsin(\lambda\hat{\mu}/2\pi d_{\text{t}})$. When $N_{\text{RF}} = 1$, $\boldsymbol{F}_{\text{RF}}$ can therefore be determined by the transmitter as [8, 9]

$$\boldsymbol{F}_{\text{RF}} = \mathbf{a}_{\text{t}}(\hat{\theta}). \tag{12}$$

In the following, we illustrate the employment of the proposed auxiliary beam pairs design for hybrid precoding. We employ a sequential algorithm which in general involves two separate steps [8]. The first step tries to find the best analog transmit beamforming vectors without respect to the digital baseband precoder. Regarding the selection of best analog transmit beamforming vectors, the following steps are executed with respect to each transmit antenna subarray:

- Step-1: each transmit antenna subarray probes auxiliary beam pairs within a given angular range.
- Step-2: according to (9), the receiver calculates a set of ratio measures with each of them corresponding to a single transmit antenna subarray. The quantized values of the ratio measures are fed back to the transmitter.
- Step-3: upon receiving the feedback from the receiver, the transmitter constructs $\boldsymbol{F}_{\text{RF}}$ with the non-zero entries in each of its column determined according to (10)∼(12).

It can be observed from Step-1 to Step-3 that, in fact, each column of $\boldsymbol{F}_{\text{RF}}$ is determined by simply iterating the proposed single RF-based auxiliary beam pairs design for all transmit antenna subarrays. Indeed, in terms of maximizing the total achievable data rate where multiple transmit antenna subarrays are involved, independently choosing the beamforming vector with respect to each transmit antenna subarray is suboptimal [18]. Thanks to the multiple RF chains equipped at the receiver, the receiver is able to construct different analog combining vectors that steer towards various angular directions for data receptions. For instance, by increasing the number of receive RF chains, and/or by jointly optimizing $\boldsymbol{W}_{\text{RF}}$ with the auxiliary beam pairs, the achievable sum rate can be maximized. Finally, the best matched baseband precoding matrix $\boldsymbol{F}_{\text{BB}}$ and combining matrix $\boldsymbol{W}_{\text{BB}}$ are determined by the receiver according to the procedures presented in [8].

4. NUMERICAL RESULTS

In this section, we evaluate the performance of the proposed auxiliary beam pairs based design approach in terms of spectral efficiency and implementation complexity. The transmitter and receiver employ ULA with inter-element spacing $\lambda/2$. The total number of antenna elements employed at the transmitter is set to be $N_{\text{tot}} = 64$. The transmitter spans $120°$ around boresight while the receiver monitors a complete $180°$ region around boresight. For the method developed in [9], the codebook for analog transmit beamforming consists of 12 beams uniformly spread in the $120°$ region, and Λ_{RF} denotes the number of bits required to feed back the selected beam index per each RF chain. In the proposed auxiliary beam pairs based hybrid precoding, the indices of the selected auxiliary beam pairs ought be fed back to the transmitter. The ratio measures are quantized as well by using codewords that are

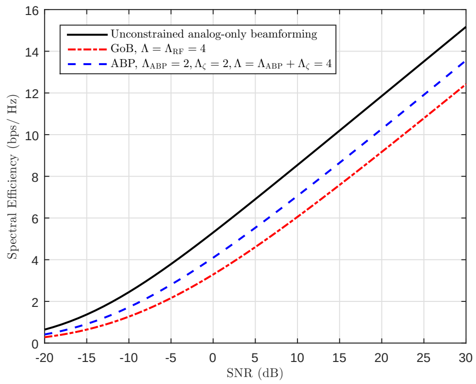

Fig. 3. Spectral efficiency performance of the grid-of-beam and the proposed auxiliary beam pairs based analog-only beamforming.

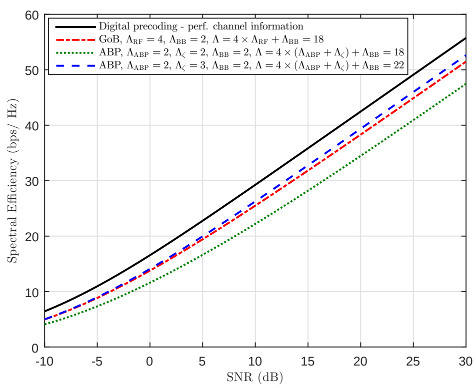

Fig. 4. Spectral efficiency performance of the grid-of-beam and the proposed auxiliary beam pairs based closed-loop hybrid precoding.

uniformly distributed within the interval $[-1, 1]$. Denote by Λ_{ABP} and Λ_{ζ} the number of feedback bits required for quantizing the index of the selected auxiliary beam pair and the ratio metric per each RF chain.

Fig. 3 shows the spectral efficiency performance of the grid-of-beam and the proposed auxiliary beam pairs based analog-only beamforming ($N_{\mathrm{RF}} = 1$). In this example, LOS channel is assumed with $M_{\mathrm{tot}} = 1$. In the auxiliary beam pairs based method, 3 auxiliary beam pairs are employed to cover the $120°$ region. The number of bits required to quantize the index of the selected auxiliary beam pair are therefore $\Lambda_{\mathrm{ABP}} = 2$. Two additional bits are used to quantize the ratio metric (i.e., $\Lambda_{\zeta} = 2$). From the evaluation results, it is observed that under the same amount of feedback bits, the proposed auxiliary beam pairs based approach exhibits better performance than the grid-of-beam in LOS channel.

Fig. 4 exhibits the spectral efficiency performance of the grid-of-beam and the proposed auxiliary beam pairs based closed-loop hybrid precoding. The digital precoding with perfect channel state information is plotted for comparison. The digital baseband precoder is selected from the 4×2 codebook employed in the LTE standard [19], and Λ_{BB} represents the number of feedback bits for digital baseband precoding. Four independently steerable antenna subarrays with 16 antenna elements each are employed at the transmitter, i.e., $N_{\mathrm{RF}} = 4$ and $N_{\mathrm{Sub}} = 16$. The total number of antenna elements employed at the receiver is 16 with only one RF chain, i.e., $M_{\mathrm{RF}} = 1$ and $M_{\mathrm{Sub}} = 16$. ITU-R urban micro (UMi) channel with NLOS small-scale parameters is employed in this example [20]. From Fig. 4, it is observed that under the same amount of feedback bits, the proposed auxiliary beam pairs based approach is inferior relative to the grid-of-beam based method. By increasing the resolution of quantizing the ratio metric, however, the proposed auxiliary beam pairs based approach shows comparable performance relative to the grid-of-beam based method.

One of the main challenges to enable closed-loop hybrid precoding is the high implementation complexity in terms of reference signal (RS) overhead and finding the best pairs of analog transmit and receive beams. For the grid-of-beam based approach, each analog beam transmitted from every antenna subarray has a distinct RS symbol to enable efficient channel estimation. Taking Fig. 4 as the example to illustrate, the number of RS symbols required by the grid-of-beam based method is $12 \times N_{\mathrm{RF}} = 48$. For the proposed auxiliary beam pairs based approach, as only 3 auxiliary beam pairs are formed, the total number of RS symbols required becomes to $6 \times N_{\mathrm{RF}} = 24$. That is, at most 50% RS overhead can be saved by employing the proposed auxiliary beam pairs based approach. The number of iterations required for the grid-of-beam based approach is computed as $12^{N_{\mathrm{RF}}} + 2^2 = 20740$ [8], while this number becomes to $6 \times N_{\mathrm{RF}} + 2^2 = 28$ for the proposed auxiliary beam pairs based method. The computational complexity scales exponentially with the number of RF chains in the grid-of-beam based method, while linearly with the number of RF chains in the proposed approach.

5. CONCLUSION

In this paper, auxiliary beam pairs design is proposed and evaluated for mmWave cellular systems to facilitate closed-loop hybrid precoding. Performance analysis and evaluation results show that by employing the custom designed pairs of analog beams, the proposed approach can remarkably reduces the implementation complexity, meanwhile achieve promising spectral efficiency performance.

6. ACKNOWLEDGEMENT

This work is sponsored by a research gift from Huawei.

7. REFERENCES

[1] Z. Pi and F. Khan, "An introduction to millimeter-wave mobile broadband systems," *IEEE Commun. Mag.*, vol. 49, pp. 101–107, June 2011.

[2] T. S. Rappaport, S. Sun, R. Mayzus, H. Zhao, Y. Azar, K. Wang, G. Wong, J.Schulz, M. Samimi, and F. Gutierrez, "Millimeter wave mobile communications for 5G cellular: It will work!," *IEEE Access*, vol. 1, pp. 335–349, May 2013.

[3] R. W. Heath Jr., N. Gonzalez-Prelcic, S. Rangan, W. Roh, and A. Sayeed, "An overview of signal processing techniques for millimeter wave MIMO systems," *Submitted to IEEE J. Sel. Top. Signal Process., arXiv preprint arXiv:1512.03007*, Dec. 2015.

[4] T. S. Rappaport, R. W. Heath Jr., R. C. Daniels, and J. N. Murdock, *Millimeter wave wireless communications*, Prentice Hall, 2014.

[5] O. E. Ayach, R. W. Heath Jr., S. Abu-Surra, S. Rajagopal, and Z. Pi, "The capabity optimality of beam steering in large millimeter wave MIMO systems," in *Intern. Workshop Signal Process. Adv. Wireless Commun. (SPAWC'12)*. IEEE, Jun. 2012, pp. 100–104.

[6] O. E. Ayach, S. Rajagopal, S. Abu-Surra, Z. Pi, and R. W. Heath Jr., "Spatially sparse precoding in millimeter wave MIMO systems," *IEEE Trans. Wireless Commun.*, vol. 13, pp. 1499–1513, March 2014.

[7] R. Mendez-Rial, C. Rusu, N. Gonzalez-Prelcic, and R. W. Heath Jr., "Dictionary-free hybrid precoders and combiners for mmWave mimo systems," in *Intern. Workshop Signal Process. Adv. Wireless Commun. (SPAWC'15)*. IEEE, 2015, pp. 151–155.

[8] T. Kim, J. Park, J.-Y. Seol, J. Cho, and W. Roh, "Tens of Gbps support with mmWave beamforming systems for next generation communications," in *Global Telecomm. Conf. (GLOBECOM'13)*. IEEE, 2013, pp. 3685–3690.

[9] C. Kim, T. Kim, and J.-Y. Seol, "Multi-beam transmission diversity with hybrid beamforming for MIMO-OFDM systems," in *Global Telecomm. Conf. (GLOBECOM'13)*. IEEE, 2013, pp. 61–65.

[10] A. Alkhateeb, O. E. Ayach, G. Leus, and R. W. Heath Jr., "Hybrid precoding for millimeter wave cellular systems with partial channel knowledge," in *Info. Theory and App. Workshop (ITA'13)*. IEEE, 2013, pp. 1–5.

[11] R. Mendez-Rial, C. Rusu, N. Gonzalez-Prelcic, A. Alkhateeb, and R. W. Heath Jr., "Hybrid MIMO architectures for millimeter wave communications: phase shifters or switches," *IEEE Access*, vol. PP, no. 99, pp. 1, Jan. 2016.

[12] E. M. Hofstetter and D. Delong, "Detection and parameter estimation in an amplitude-comparison monopulse radar," *IEEE Trans. Inf. Theory*, vol. 15, no. 1, pp. 22–30, Jan. 1969.

[13] J. D. Glass and W. D. Blair, "Monopulse DOA estimation using adjacent matched filter samples," in *Aerospace conference*. IEEE, 2015, pp. 1–8.

[14] F. Yuan, G. P. Villardi, F. Kojima, and H. Yano, "Channel direction information probing for multi-antenna cognitive radio system," in *Tech. Rep.* IEICE, May 2015, vol. 115, pp. 39–44.

[15] N. H. Adams, H. B. Sequeira, M. Bray, D. Srinivasan, R. Schulze, S. Berman, and H. Ambrose, "Monopulse autotrack methods using software-defined radios," in *Aerospace conference*. IEEE, 2015, pp. 1–6.

[16] H. Xu, V. Kukshya, and T. S. Rappaport, "Spatial and temporal characteristics of 60-GHz indoor channels," *IEEE J. Sel. Areas Commun.*, vol. 20, no. 3, pp. 620–630, Apr. 2002.

[17] Z. Muhi-Eldeen, L. Ivrissimtzis, and M. Al-Nuaimi, "Modelling and measurements of millimeter wavelength propagation in urban environments," *IET Microwaves, Antennas & Propagation*, vol. 4, no. 9, pp. 1300–1309, 2010.

[18] X. Gao, L. Dai, S. Han, C.-L. I, and R. W. Heath Jr., "Energy-efficient hybrid analog and digital precoding for mmWave MIMO systems with large antenna arrays," *Submitted to IEEE Trans. Wireless Commun., arXiv preprint arXiv:1507.04592*, Jul. 2015.

[19] "Technical Specification Group RAN: Evolved Universal Terrestrial Radio Access (E-UTRA); Physical Channels and Modulation," 3GPP, Dec. 2011. [Online]. Available: http://www.3gpp.org/ftp/Specs/html-info/36211.htm.

[20] "Guidelines for evaluation of radio interface technologies for IMT-Advanced," Technical Report, ITU-R M.2135.